Tunnelling piezoresistive effect of grain boundary in polysilicon nano-films*

Chuai Rongyan(揣荣岩)[1,†], Liu Bin(刘斌)[1], Liu Xiaowei(刘晓为)[2], Sun Xianlong(孙显龙)[1], Shi Changzhi(施长治)[2], and Yang Lijian(杨理践)[1]

(1 Information Science and Engineering School, Shenyang University of Technology, Shenyang 110023, China)
(2 Department of Microelectronics, Harbin Institute of Technology, Harbin 150001, China)

Abstract: The experiment results indicate that the gauge factor of highly boron doped polysilicon nanofilm is bigger than that of monocrystalline silicon with the same doping concentration, and increases with the grain size decreasing. To apply the unique properties reasonably in the fabrication of piezoresistive devices, it was expounded based on the analysis of energy band structure that the properties were caused by the tunnel current which varies with the strain change forming a tunnelling piezoresistive effect. Finally, a calculation method of piezoresistance coefficients around grain boundaries was presented, and then the experiment results of polysilicon nanofilms were explained theoretically.

Key words: polysilicon nanofilm; tunnelling piezoresistive effect; gauge factor; piezoresistance coefficient
DOI: 10.1088/1674-4926/31/3/032002 **PACC:** 7220F; 7360F; 7340G

1. Introduction

The discovery[1] in 1974 that the polysilicon thin films have piezoresistive properties generated considerable research into an increasing number of applications in piezoresistive sensors. Therefore, the investigations into their piezoresistive mechanism have attracted great attention. The existing piezoresistive models of polysilicon were established during 1980s–1990s, which were widely applied in the design and optimization of polysilicon pressure sensors[2]. In the 1980's, French and Evans considered both thermionic emission and diffusion as conducting mechanisms of polysilicon and their sensitivity to strain, and then presented a model valid over a wide range of doping concentrations[3−5]. In their theory, the piezoresistance coefficient of grain boundaries was much lower than that of grains, resulting in the fall of gauge factor at high doping concentrations. Thus, the conclusion was drawn that larger grain sizes and low trap densities yielded a higher gauge factor. Meanwhile, Schubert took the influences of depletion regions and grain boundaries into consideration and proposed a theoretical model for calculating the longitudinal and transversal gauge factors[6]. Also, the maximum gauge factor was obtained in polysilicon films with large grain sizes. In view of the above conclusions, at present, the thickness of polysilicon films used in piezoresistive devices is mostly over 200 nm, and even larger than 1 μm in some cases. Few polysilicon nanofilms (around or less than 100 nm in thickness) are adopted for sensing applications, due to their extremely fine grain sizes and deficient crystallization. In these existing piezoresistive models, it is considered that the piezoresistive effect of grain neutral regions is stronger than that of grain boundaries. Therefore, when the grain size is fine, the proportion of the latter becomes large relatively, and the piezoresistive effect should be weakened accordingly.

However, the above deduction from the existing models was based on the test results of polysilicon films thicker than 200 nm, but opposite to the actual experiment results of polysilicon nanofilms. The polysilicon nanofilms exhibit excellent piezoresistive properties, which show potential for the fabrication and development of high performance piezoresistive sensors. In this paper, in order to analyze the piezoresistive properties of polysilicon nanofilms, we prepared the 80-nm-thick polysilicon films with different doping concentrations and a series of polysilicon films with various thicknesses. By analyzing the energy band structure and transport current components through grain boundaries, the relationship between piezoresistance coefficients of grain neutral regions and composite grain boundaries was obtained and the tunnelling piezoresistive effect of polysilicon nanofilms differing from common polysilicon films was presented and analyzed. Finally, the experimental results of polysilicon nanofilms were explained theoretically.

Additionally, the piezoresistive effect derived from the tunnelling current—tunnelling piezoresistive effect—was not mentioned before. Although the view that the tunnelling current could generate a piezoresistive effect was accepted by Kleimann *et al.*[7], the regularity of tunnelling piezoresistive effect and its influence on the piezoresistive properties of polysilicon have not been revealed, as a result of the complexity of tunnelling current formulas.

2. Basic experimental phenomenon

For the first group samples, the 80-nm-thick polysilicon films were prepared on ⟨111⟩-orientated thermally oxidized silicon substrates by LPCVD at 620°. After the boron implantation, the annealing step was performed at 1080° for 30 min, and the boron doping concentration was ranged from 8.1×10^{18} to 7.1×10^{20} cm^{-3}. Another group of polysilicon films (30–250 nm in thickness) were deposited on thermally oxidized silicon substrates using the same process and temperature. After boron

* Project supported by the National Natural Science Foundation of China (No. 60776049), the Science and Technology Foundation of Liaoning Province of China (No. 20072036), and the Fund of Liaoning Province Education Department of China (No. 2007T130).
† Corresponding author. Email: me_sut@163.com
Received 30 July 2009, revised manuscript received 30 September 2009

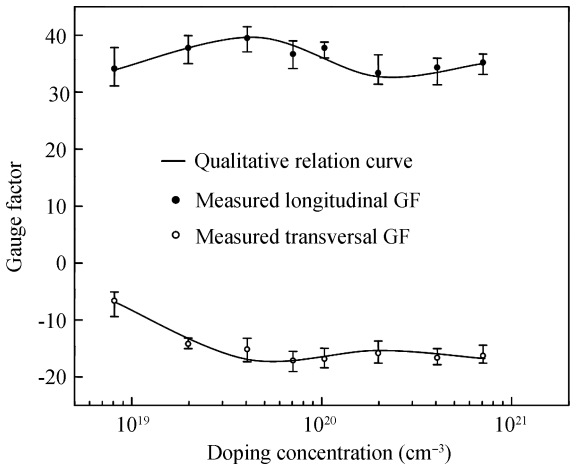

Fig. 1. Test results of the relationship between the gauge factor G_p and the doping concentration at room temperature (film thickness: 80 nm).

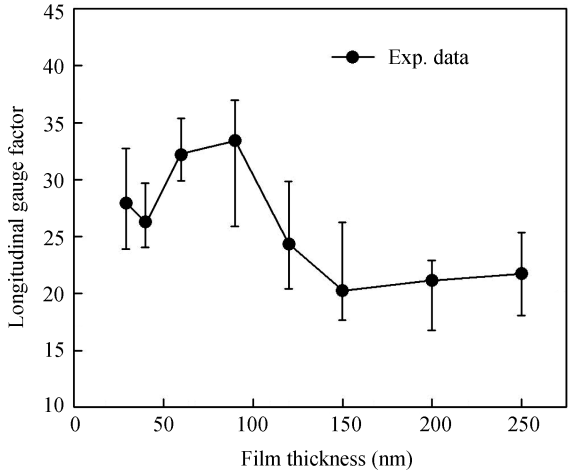

Fig. 2. Relationship between the longitudinal gauge factor G_{pl} of polysilicon and the film thickness at room temperature (doping concentration: 2.3×10^{20} cm^{-3}).

diffusion, the doping concentration of the second group was estimated to be 2.3×10^{20} cm^{-3}.

By the characterization of film microstructure, it was found that the apparent grain sizes of the first group were approximately 32 nm and the grain sizes of the second group decreased gradually from 60 to 15 nm with the film thickness varying from 250 to 30 nm[8]. To measure piezoresistive parameters, these samples were processed to obtain cantilever beams[9], and then the test results of the gauge factor were shown in Figs. 1 and 2 respectively. Seen from Fig. 1, when the doping concentration exceeded 10^{20} cm^{-3}, the gauge factor G_p ascended again with the doping concentration increasing. However, it is accepted commonly in the existing piezoresistive model that the gauge factor of polysilicon films reaches the maximum when the doping concentration is elevated to 2×10^{19} cm^{-3} approximately, and then it decreases monotonously with the doping concentration increasing[2, 3]. The test results shown in Fig. 2 indicated that the gauge factor increased remarkably when the film thickness reduced from 150 to 90 nm, in despite of the distinct decrease of grain size. Obviously,

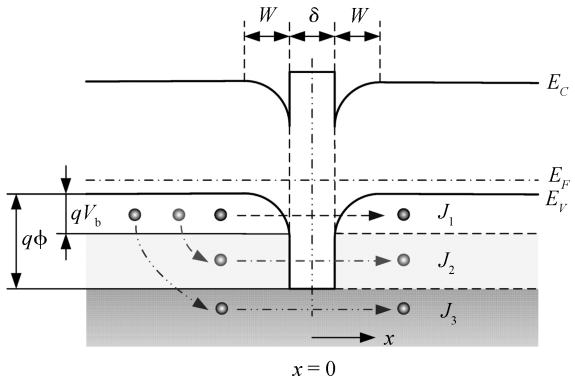

Fig. 3. Energy band diagrams near a grain boundary under thermal equilibrium.

these phenomena can not be explained by the existing piezoresistive models of polysilicon. The reason is that the piezoresistive effect of the grain boundary is underestimated in the existing models.

3. Energy band diagram and equivalent circuit of polysilicon

The polysilicon could be regarded as being composed of small crystallites joined together by grain boundaries. In order to analyze the influence of tunnelling effect on the conduction properties of polysilicon, the grain boundary is viewed as a disordered amorphous material, and the forbidden band width is much larger than that of monocrystalline silicon and approaches that of amorphous silicon (1.5–1.6 eV) [10−12], and the Fermi level is pinned near the midgap at grain boundaries. As a result, a heterojunction is formed at the interface between the crystallites and the grain boundary. For the sake of simplification, a one dimensional ideal conduction model for polysilicon was used. In this model, it is assumed that the distribution of grain boundaries is homogeneous, and the grains serve as a series of cubes (the length of side is L) arranged in the one-dimensional mode.

Based on the above assumption, the energy band diagram around the grain boundaries was given in Fig. 3, where W is the depletion region width, δ is the grain boundary width, $q\phi$ is the height of grain boundary barrier, and qV_b is the height of depletion region barrier. For the holes traversing grain boundaries, when the kinetic energy E_x is less than qV_b, they can traverse the depletion regions and boundary barrier region only by tunneling, forming the field emission current J_1; when $qV_b < E_x < q\phi$, they cross the depletion regions by thermal emission and penetrate the boundary barrier region by tunneling, forming the composite current J_2; when $E_x > q\phi$, they traverse the depletion regions and boundary barrier region completely by thermal emission, forming the thermal emission current J_3.

Sequentially, by synthesizing the above three current modes, the equivalent circuit of polysilicon is presented in Fig. 4(a), where R_g is the resistance of grain neutral regions, R_F and R_T are the resistances determined by the currents J_1 and J_3, respectively. For the current J_2, the composite current path was equated with two series resistances. One is the equivalent emission resistance R_d of depletion regions determined

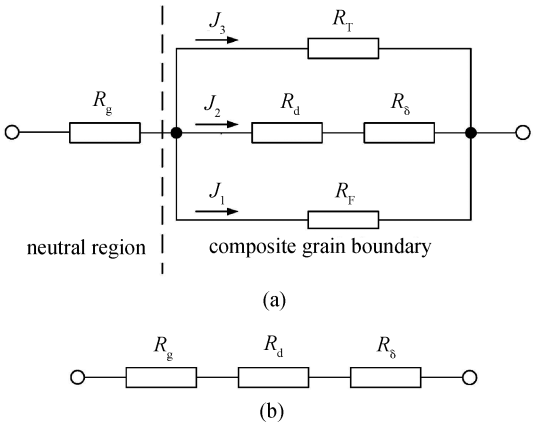

Fig. 4. Equivalent circuit of tunnel piezoresistive model. (a) The general form. (b) The simplified form at a moderate temperature.

by thermal emission; the other is the equivalent tunnelling resistance R_δ of grain boundary determined by tunnelling. Although these three current modes coexist in polysilicon, the current J_2 is dominated for the samples with high doping concentration at room temperature. Hence, the equivalent circuit can be simplified into the form given in Fig. 4(b).

According to Fig. 4(b), the expression of gauge factor for polysilicon is given by

$$G_p = \frac{R_g}{R_g + R_b} G_g + \frac{R_b}{R_g + R_b} G_b, \tag{1}$$

where G_g and G_b are the gauge factors of the resistances R_g and R_b, respectively; R_b is the resistance of composite grain boundary comprised of grain boundary and depletion regions, and $R_b = R_d + R_\delta$.

Inside each grain, atoms are arranged in a monocrystallite mode, and the gauge factor of grain neutral regions is dependent on the piezoresistance coefficient π_g of monocrystalline silicon. The gauge factor G_b is dependent on the piezoresistance coefficients of equivalent resistances R_d and R_δ. For the equivalent resistance R_d, using the dependence of the thermal emission current on strain, the relational expressions of the longitudinal and transversal piezoresistance coefficients π_{dl} and π_{dt} in [111] orientation are given by[13]

$$\pi_{dl} = 0.525\pi_{gl}, \tag{2}$$

$$\pi_{dt} = 0.616\pi_{gt}, \tag{3}$$

where π_{gl} and π_{gt} are the longitudinal and transversal piezoresistance coefficients of p-type monocrystalline silicon in $\langle 111 \rangle$ orientation, respectively. The resistance ratio in Eq. (1) can be figured out by the corresponding voltage drop ratio. Nevertheless, calculating G_p requires determining the piezoresistance coefficient π_δ of the equivalent tunnel resistance R_δ.

4. Piezoresistive properties of grain boundary

Before analyzing piezoresistive properties of composite grain boundary, the volt-ampere characteristics of the resistance R_δ should be determined. The resistance R_δ is defined as the grain boundary resistance without regard to depletion regions. Figure 5 is the energy band diagram around grain boundary related to the resistance R_δ under the voltage drop V_δ. Using Fermi–Dirac statistics, the number of holes having energy within the range dE_x incident from left to right on the grain boundary barrier per unit time per unit area is[14]

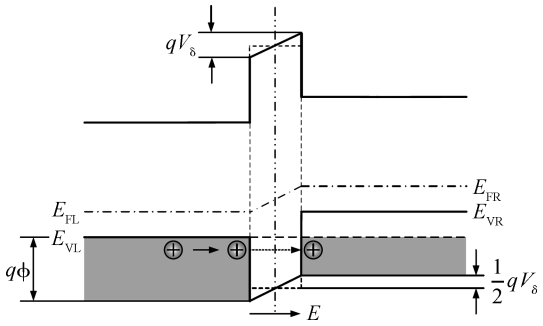

Fig. 5. Energy band diagram near a grain boundary without regard to depletion region barriers.

$$N(T, \xi, E_x)dE_x = \frac{4\pi m_d kT}{h^3} \times \ln\left(1 + \exp\left[\frac{-(E_x + \xi)}{kT}\right]\right) dE_x, \tag{4}$$

where m_d is the effective mass of holes for state density, $\xi = E_F - E_V$, is the difference of Fermi level and valence band edge, h is Planck's constant, k is Boltzmann's constant, and T is the absolute temperature.

The grain boundary width in polysilicon is very small (around 1nm in general), and the number of holes with high energies around $q\phi$ is few. Hence, when calculating the current density, the oblique distribution of energy band at the top of grain boundary barrier in Fig. 5 can be substituted by the horizontal line approximately. So, the probability of carriers with the energy E_x ($0 \leqslant E_x \leqslant q\phi - \frac{1}{2}qV_\delta$) tunnelling the grain boundary barrier is given by

$$D(E_x) = \exp\left\{\frac{-4\pi\delta}{h}\left[2m_i(a - E_x)\right]^{1/2}\right\}, \tag{5}$$

$$a = q\phi - \frac{1}{2}qV_\delta, \tag{6}$$

where m_i is the effective mass of holes in the tunnelling direction. In Fig. 5, the left valence band edge E_{VL} is taken to be the zero point of energy. Therefore, by deducing from Eqs. (4)–(6), the hole-flux density tunnelling grain boundary barrier from left to right is

$$S_{LR} = \int_0^a N(T, \xi, E_x) D(E_x) dE_x. \tag{7}$$

It is obvious that the holes with energies less than E_{VL} could not tunnel the barrier from right to left. Thus, the hole-flux density tunneling grain boundary barrier from right to left is written as

$$S_{RL} = \int_0^a N(T, \xi', E_x) D(E_x) dE_x, \tag{8}$$

$$\xi' = \xi + qV_\delta. \tag{9}$$

In the nondegenerate condition ($\xi \gg kT$), the logarithmic function term in Eq. (1) can be simplified into the exponential form, and then Equation (7) can be expressed as

$$S_{\mathrm{LR}} = \frac{4\pi m_{\mathrm{d}} kT}{h^3} \int_0^a \exp\left[\frac{-(E_{\mathrm{x}} + \xi)}{kT}\right] D(E_{\mathrm{x}}) \mathrm{d}E_{\mathrm{x}}. \quad (10)$$

Owing to the fact that the holes gather mostly near the valence band edge, when solving the integration in Eq. (10), the square root term is expended by the Taylor's series as follows:

$$(a - E_{\mathrm{x}})^{1/2} = \sqrt{a} - \frac{E_{\mathrm{x}}}{2\sqrt{a}} + \cdots. \quad (11)$$

After Equation (11) is substituted into Eq. (5), the yielded $D(E_{\mathrm{x}})$ expression is substituted into Eq. (10). By integration, it results in

$$S_{\mathrm{LR}} = \frac{4\pi m_{\mathrm{d}} k^2 T^2}{h^3 c_1} \left[\exp\left(-\frac{2\pi\delta}{h}\sqrt{2m_{\mathrm{i}}a} - \frac{a+\xi}{kT}\right) - \exp\left(-\frac{4\pi\delta}{h}\sqrt{2m_{\mathrm{i}}a} - \frac{\xi}{kT}\right)\right], \quad (12)$$

where

$$c_1 = \frac{2\pi\delta}{h} kT \sqrt{\frac{2m_{\mathrm{i}}}{a}} - 1. \quad (13)$$

In like manner, it can yield

$$S_{\mathrm{RL}} = \frac{4\pi m_{\mathrm{d}} k^2 T^2}{h^3 c_1} \left[\exp\left(-\frac{2\pi\delta}{h}\sqrt{2m_{\mathrm{i}}a} - \frac{a+\xi'}{kT}\right) - \exp\left(-\frac{4\pi\delta}{h}\sqrt{2m_{\mathrm{i}}a} - \frac{\xi'}{kT}\right)\right]. \quad (14)$$

From Eqs. (12) and (13), the current density of tunnelling boundary barrier region can be given by

$$\begin{aligned} J_\delta &= q(S_{\mathrm{LR}} - S_{\mathrm{RL}}) \\ &= q\frac{4\pi m_d k^2 T^2}{h^3 c_1} \exp\left(-\frac{\xi}{kT}\right) \\ &\quad \times \left[\exp\left(c_2 - \frac{a}{kT}\right) - \exp\left(c_2 - \frac{a+qV_\delta}{kT}\right) - \exp(2c_2) + \exp\left(2c_2 - \frac{qV_\delta}{kT}\right)\right], \end{aligned} \quad (15)$$

where

$$c_2 = -\frac{2\pi\delta}{h}\sqrt{2m_{\mathrm{i}}a}. \quad (16)$$

On the condition of low voltage bias ($qV_\delta \ll kT$), the exponential terms in Eq. (15) can be expanded by using the Taylor's series. After taking the first order approximation, it yields

$$J_\delta = \frac{4\pi q^2 m_{\mathrm{d}} kT}{h^3 c_1} \exp\left(-\frac{\xi_{\mathrm{p}}}{kT}\right) \times \left[\exp\left(c_2 - \frac{a}{kT}\right) - \exp(2c_2)\right] V_\delta. \quad (17)$$

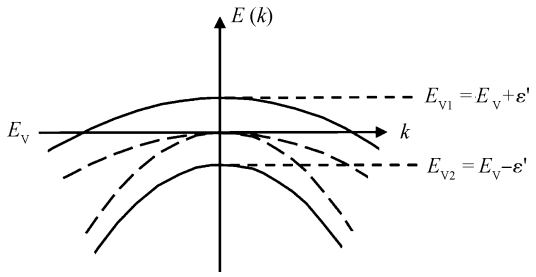

Fig. 6. Split off of valence bands subjected to a uniaxial stress.

Considering the hole concentration formula in nondegenerate semiconductor[15]:

$$p = N_{\mathrm{V}} \exp\left(\frac{-\xi}{kT}\right) = 2\left(\frac{2\pi m_{\mathrm{d}} kT}{h^2}\right)^{\frac{3}{2}} \exp\left(\frac{E_{\mathrm{V}} - E_{\mathrm{F}}}{kT}\right), \quad (18)$$

and then Equation (17) can be rewritten as

$$\begin{aligned} J_\delta &= \frac{pq}{c_1}\left(\frac{kT}{2\pi m_{\mathrm{d}}}\right)^{1/2} \left[\exp\left(c_2 - \frac{a}{kT}\right) - \exp(2c_2)\right], \\ \frac{qV_\delta}{kT} &= pJ_{\delta 0}. \end{aligned} \quad (19)$$

The valence band edge E_{V} of silicon consists of two degenerate energy bands. Therefore, the tunnelling current of traversing grain boundary is comprised of the corresponding hole tunnelling current $J_{\delta 1}$ and $J_{\delta 2}$, and can be expressed by

$$J_\delta = \sum_{j=1}^{2} J_{\delta \mathrm{j}} = J_{\delta 1} + J_{\delta 2}, \quad (20)$$

$$J_{\delta j} = p_{\mathrm{j}} (J_{\delta 0})_{\mathrm{j}}, \quad (21)$$

where $J_{\delta \mathrm{j}}$ is the tunnelling current component of degenerate energy band, p_{j} is the corresponding hole concentration, $j = 1, 2$, corresponds to two sorts of holes.

4.1. Piezoresistance coefficient of equivalent tunnel resistance

The grain neutral region has the nature of monocrystalline silicon, and its piezoresistive properties are considered as a result of the split off of two degenerate bands subjected to a stress[16, 17]. One of the two bands, E_{V1}, is shifted upward; the other band, E_{V2}, is shifted downward. The band shift ε' is defined as the strain additional energy, as shown in Fig. 6.

When subjected to a uniaxial stress, the isoenergetic surfaces of two split-off bands in the k space become the rotation ellipsoid surfaces, the symmetry axis of which is in the stress direction. For simplification, the case that a uniaxial stress is applied along ⟨111⟩ orientation is analyzed. According to the result of the cyclotron resonance experiment by Hensel and Feher[18], the effective mass of holes under a strong stress is obtained in Table 1, where m_{lj} and m_{tj} are the longitudinal and transversal effective mass of holes at the band E_{Vj}, respectively.

When the crystal is applied by a stress, two valence band edges are split off and become $E_{\mathrm{V}} + \varepsilon'$ and $E_{\mathrm{V}} - \varepsilon'$, respectively. For the nondegenerate p-type silicon, it is assumed that

Table 1. Hole effective mass in highly stressed silicon (unit: free-electron mass m_0).

Parameter	Value
m_{l1}	0.870
m_{t1}	0.170
m_{d1}	0.293
m_{l2}	0.135
m_{t2}	0.369
m_{d2}	0.264

the Fermi level is constant for stress. After differentiating Eq. (18) and substituting $\mathrm{d}E_V$ by the strain additional energy ε', the concentration changes of two sorts of holes are, respectively:

$$\Delta p_1 = N_{v1} \exp\left(\frac{E_V - E_F}{kT}\right)\frac{\varepsilon'}{kT}, \tag{22}$$

$$\Delta p_2 = -N_{v2} \exp\left(\frac{E_V - E_F}{kT}\right)\frac{\varepsilon'}{kT}. \tag{23}$$

When the uniaxial stress is $\bar{\sigma}$, the additional energy of band split-off is[18, 19]

$$\varepsilon' = \frac{1}{3} D_u C_{44}^{-1} \bar{\sigma}, \tag{24}$$

where D_u is deformation potential constant, C_{44} is the corresponding elastic stiffness constant.

Due to the different effective mass of two sorts of holes, the change of the corresponding hole concentrations consequentially results in the change in the current J_δ, thereby leading the resistance R_δ to change accordingly—it is the mechanism of tunnelling piezoresistive effect. The relative change of resistivity for tunnelling piezoresistive effect is

$$\frac{\Delta\rho_\delta}{\rho_\delta} = -\frac{\Delta J_\delta}{J_\delta} = -\frac{\Delta p_1 (J_{\delta 0})_1 + \Delta p_2 (J_{\delta 0})_2}{p_1 (J_{\delta 0})_1 + p_2 (J_{\delta 0})_2}. \tag{25}$$

By combining Eqs. (18), (22), (23) and (25), it yields

$$\frac{\Delta\rho_\delta}{\rho_\delta} = \frac{1 - \left(\dfrac{m_{d1}}{m_{d2}}\right)^{3/2} \dfrac{(J_{\delta 0})_1}{(J_{\delta 0})_2}}{1 + \left(\dfrac{m_{d1}}{m_{d2}}\right)^{3/2} \dfrac{(J_{\delta 0})_1}{(J_{\delta 0})_2}} \frac{\varepsilon'}{kT}. \tag{26}$$

According to Eqs. (19)–(21), it results in

$$\frac{(J_{\delta 0})_1}{(J_{\delta 0})_2} = \frac{(c_1)_2 \left\{ \exp\left[(c_2)_1 - \dfrac{a}{kT}\right] - \exp\left[2\,(c_2)_1\right] \right\}}{(c_1)_1 \left\{ \exp\left[(c_2)_2 - \dfrac{a}{kT}\right] - \exp\left[2\,(c_2)_2\right] \right\}}, \tag{27}$$

where $(c_1)_j$ and $(c_2)_j$ are a couple of constants for calculating the tunnelling current component of holes at the band E_{Vj} and determined by Eqs. (13) and (16), respectively. For the longitudinal piezoresistive effect along ⟨111⟩ orientation, using the longitudinal effect mass m_{l1} in Table 1, $(c_1)_1$ and $(c_2)_1$ are calculated to be −0.84 and −3.72, respectively; using the longitudinal effect mass m_{l2}, $(c_1)_2$ and $(c_2)_2$ are equal to −0.94 and –1.46, respectively. Referring to the experimental data provided by Mandurah[10] during the analysis of the conduction properties of polysilicon, the grain boundary width δ is taken to be 1 nm and the grain boundary barrier height $q\phi$ is about 0.6 eV. Usually, $qV_\delta \ll q\phi$, and from Eq. (6), it can be obtained that $a \approx q\phi$. Hence, using the data in Table 1 and Eq. (27), it results in

$$\left(\frac{m_{d1}}{m_{d2}}\right)^{3/2} = \sqrt{\frac{m_{l1} m_{t1}^2}{m_{l2} m_{t2}^2}} = 1.180, \tag{28}$$

$$\frac{(J_{\delta 0})_1}{(J_{\delta 0})_2} = 1.22 \times 10^{-2}. \tag{29}$$

Using Eqs. (24), (26)–(29), the longitudinal piezoresistance coefficient of the resistance R_δ along ⟨111⟩ orientation is

$$\pi_{\delta l} = \frac{\Delta\rho_\delta}{\rho_\delta \bar{\sigma}} = \frac{0.972}{3} D_u C_{44}^{-1} \frac{1}{k_0 T}. \tag{30}$$

Similarly, the transversal piezoresistance coefficient along ⟨111⟩ orientation is

$$\pi_{\delta t} = \frac{\Delta\rho_\delta}{\rho_\delta \bar{\sigma}} = \frac{-0.684}{3} D_u C_{44}^{-1} \frac{1}{k_0 T}. \tag{31}$$

Under the uniaxial stress $\bar{\sigma}$ applied along ⟨111⟩ orientation, the longitudinal and transversal piezoresistance coefficients (for grain neutral regions) of p-type monocrystalline silicon can be expressed as follows, respectively[13]:

$$\pi_{gl} = \frac{0.695}{3} D_u C_{44}^{-1} \frac{1}{k_0 T}, \tag{32}$$

$$\pi_{gt} = -\frac{0.435}{3} D_u C_{44}^{-1} \frac{1}{k_0 T}. \tag{33}$$

Comparing Eqs. (30) and (31) with (32) and (33) accordingly, it yields

$$\pi_{\delta l} = 1.4\pi_{gl}, \tag{34}$$

$$\pi_{\delta t} = 1.6\pi_{gt}. \tag{35}$$

The above derivation is performed for a nondegenerate semiconductor. As to the degenerate semiconductor, the difference of the calculating formulas of carrier concentration could result in the change of piezoresistive coefficients. However, the influences of this change on the resistance R_g and the resistance R_δ are identical. Therefore, in the degenerate case, the ratio of piezoresistance coefficients π_δ and π_g is invariable, still determined by Eqs. (34) and (35). That is, no matter the degenerate or nondegenerate semiconductor, the piezoresistance coefficients π_δ and π_g always keep a uniform proportional relationship. Moreover, the piezoresistance coefficient π_δ is larger than π_g remarkably.

4.2. Piezoresistance coefficient of composite grain boundary

The resistances R_d and R_δ in Fig. 4(b) are two abstract equivalent resistances. Although they appear to be in series, they belong to the same physical space within the film actually, resulting in the resistivity of the composite grain boundary being equal to the resistivity sum of two equivalent resistances, $\rho_b = \rho_d + \rho_\delta$. Thus, when the geometrical piezoresistive effect

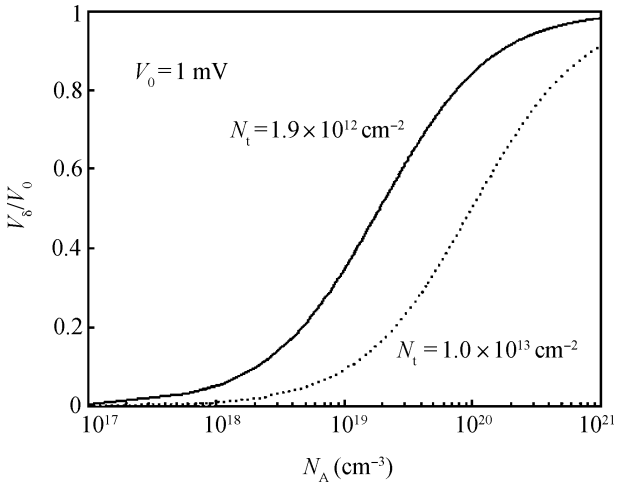

Fig. 7. Normalized distribution of voltage drop applied to grain boundaries as a function of doping concentration.

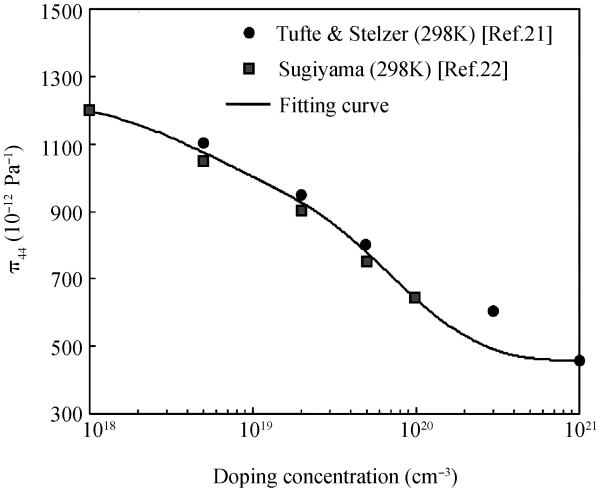

Fig. 8. Shear piezoresistance coefficient π_{44} data points and fitting curve of p-type monocrystalline silicon with different doping concentrations.

is neglected, the piezoresistance coefficient of composite grain boundary π_b can be expressed as

$$\pi_b = \frac{\Delta\rho_b}{\rho_b\bar{\sigma}} = \frac{\rho_d}{\rho_b}\frac{\Delta\rho_d}{\rho_d\bar{\sigma}} + \frac{\rho_\delta}{\rho_b}\frac{\Delta\rho_\delta}{\rho_\delta\bar{\sigma}} = \frac{R_d}{R_b}\pi_d + \frac{R_\delta}{R_b}\pi_\delta. \quad (36)$$

If the potential drops across depletion regions on the left and right hand sides of the grain boundary are denoted by V_L and V_R, respectively, then the potential drops on the resistance R_d and R_δ are $V_L + V_R$ and V_δ, respectively. Therefore, Equation (36) can be expressed as follows:

$$\pi_b = \frac{V_L + V_R}{V_0}\pi_d + \frac{V_\delta}{V_0}\pi_\delta, \quad (37)$$

$$V_0 = V_\delta + V_L + V_R. \quad (38)$$

where V_0 is the potential drop over the complete grain boundary region. Thus, it can be seen that determining the proportional relationship between $V_L + V_R$ and V_δ is the key to figure out the piezoresistance coefficient π_b.

As a piezoresistive material, the polysilicon films usually work under low current and low voltage bias, so the condition of $V_L + V_R < 4V_b$ can be always satisfied. With this understanding, Mandurah[10] colligated the theories presented by Baccarani[20] and Fonash[21], and gained the relationship of V_L, V_R, V_b and V_δ as follows:

$$2V_b^{1/2} = (V_b + V_R)^{1/2} + (V_b - V_L)^{1/2}, \quad (39)$$

$$V_\delta = \delta\left(\frac{qN_A}{2\varepsilon_s\varepsilon_0}\right)^{1/2}\left[(V_b + V_R)^{1/2} - (V_b - V_L)^{1/2}\right]. \quad (40)$$

According to the approximation of depletion region, it yields

$$V_b = \frac{qN_AW^2}{2\varepsilon_s\varepsilon_0}, \quad (41)$$

$$W = \frac{N_t}{2N_A}, \quad (42)$$

where N_A is the boron doping concentration, N_t is the trap density at grain boundary, ε_s and ε_0 are the relative dielectric constant of silicon and vacuum dielectric constant, respectively.

Using Eqs. (37)–(41), the relationship between V_L, V_R and V_δ can be resolved. Figure 7 provides the distribution of the voltage V_δ normalized to the voltage V_0 as a function of N_A, where the dashed line denotes the distribution curve of common polysilicon film with biggish film thickness, and the trap density N_t is taken to be the value of 1.9×10^{12} cm^{-2} provided by Lu[22]; the solid line denotes the distribution curve of the first group samples, the trap density N_t is taken to be 1.0×10^{13} cm^{-2}.

By substituting the relational expressions of longitudinal piezoresistance coefficients in Eqs. (2), (3), (34) and (35) into Eq. (36), the relationship between longitudinal piezoresistance coefficients of composite grain boundary (π_{bl}) and grain neutral region (π_{gl}) is

$$\pi_{bl} = 0.525\left(1 - \frac{V_\delta}{V_0}\right)\pi_{gl} + 1.40\frac{V_\delta}{V_0}\pi_{gl}. \quad (43)$$

Using Eq. (43) and the relational curve in Fig. 7, the dependence of the piezoresistance coefficient π_{bl} on N_A can be obtained. However, the piezoresistance coefficient π_{gl} along $\langle 111\rangle$ orientation must be known first. For p-type monocrystalline silicon, $\pi_{11} + 2\pi_{12} \ll 2\pi_{44}$, so yields[23]:

$$\pi_{gl} = 2\pi_{44}/3. \quad (44)$$

Here, according to the experiment results presented by Tufte & Stelzer[24] and Sugiyama[25], the fitting curve of the shear piezoresistance coefficient π_{44} of monocrystalline silicon on N_A is provided in Fig. 8. The fitting relationship between π_{44} and N_A is

$$\pi_{44} = 307.44\exp(-7.41 \times 10^{-21}N_A) + 311.03 \times \exp(-2.02 \times 10^{-20}N_A) + 178.65\exp(-2.74 \times 10^{-19}N_A) + 452.45. \quad (45)$$

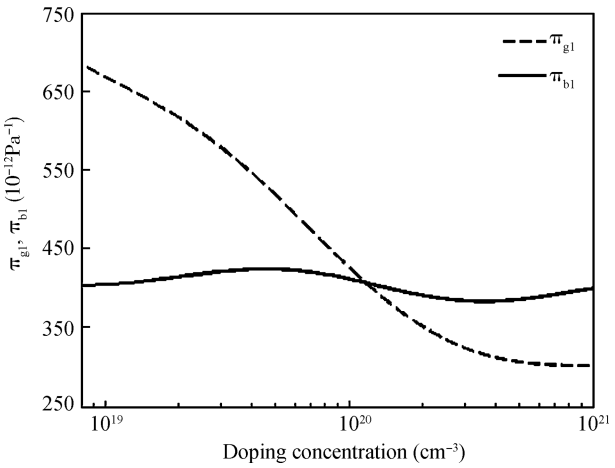

Fig. 9. Piezoresistance coefficients π_{gl} and π_{bl} as a function of doping concentration.

Consequently, using Eqs. (42) and (44) and the relational curve in Fig. 7, the dependence of the piezoresistance coefficient π_{bl} in polysilicon nanofilms on N_A is shown in Fig. 9.

It can be seen from Fig. 9 that the change regularity of the piezoresistance coefficient π_{bl} with N_A is complicated, but the change amplitude is smaller than that of the monocrystal grain. Moreover, the piezoresistance coefficient π_{bl} is larger than that of the monocrystal grain at a high doping concentration, which is the ultimate origin that polysilicon nanofilms possess a fairly large piezoresistance coefficient at a high doping concentration.

5. Comparison between theory and experiments

5.1. Gauge factor versus doping concentration

From the test results in Fig. 1, it illustrates that the gauge factor increases again with N_A increasing, after N_A reaches 2×10^{20} cm^{-3}. The phenomenon only exists in the polysilicon films with fine grains. If the grain size is large, the resistance of grain boundaries R_b will be much lower than that of grain neutral regions R_g. In this case, although the tunnelling piezoresistive effect is strong, its influence on the piezoresistive properties of polysilicon can be ignored. For the first group samples, the film thickness was 80 nm, the apparent grain sizes were 32 approximately. By comparison between the measured film resistivity and monocrystalline silicon resistivity at the same doping level, it is considered that the resistances R_g and R_b are at the same level when N_A reached 10^{20} cm^{-3}. Here, the resistance R_g decreases linearly with N_A increasing, while the change in the resistance R_b is much gentler. It results from this that the width of depletion regions could be neglected at high doping concentrations, and the width of composite grain boundaries approaches that of grain boundaries and no longer decreases with N_A increasing. Therefore, with N_A increasing, the piezoresistance coefficient of polysilicon is obviously close to that of composite grain boundaries, thereby resulting in the piezoresistance coefficient of polysilicon increasing with N_A increasing.

5.2. Analysis on test results of samples with different film thickness

According to the results observed from SEM images and XRD patterns of the second group samples[7], the dependence of gauge factor on film thickness shown in Fig. 2 indicates that: (a) When the film thickness is reduced from 250 to 150 nm, the average grain size is always around 60 nm and almost does not change, and there is a faint decrease for the measured gauge factor and the value is 22 approximately. In this case, the grain orientation of samples changes gradually from a faint ⟨110⟩ preferred orientation to a randomly oriented grain distribution. Referring to the calculating results provided by Schubert[6], the gauge factor ratio of the ⟨110⟩ preferred orientation and the random orientation is about 10/8.3. Consequently, the phenomenon that the gauge factor decreases faintly with the film thickness reducing is due to the change in grain orientation. (b) After the film thickness is reduced to 120 nm, the grain size begins to decrease remarkably with the film thickness decreasing, whereas the gauge factor increases notably; when the film thickness decreases to 90 nm, the grain size descends to 32 nm approximately, and the gauge factor reaches 33; then, the film thickness is further reduced to 60 nm, but the grain size does not change foundationally, and the gauge factor almost does not change as well. (c) When the film thickness is reduced to 40 nm, the grain size decreases to around 25 and the gauge factor descends to 27 accordingly; when the film thickness is reduced to 30 nm, the grain size becomes smaller and about 15 nm, but the gauge factor increases a little.

It could be seen from the experiment results (a) and (b) that as long as the grain size does not change, the gauge factor will not change with film thickness. Hence, the change in gauge factor is not due to the nano size effect of film thickness but is actually caused by the change in grain size. For the samples in this paper, the grain size is smaller than the film thickness. The grain size becomes the major factor determining the piezoresistive effect, thus the film thickness just indirectly influences the piezoresistive effect by the change of grain size. Therefore, when the tunnelling piezoresistive effect is discussed, the influence of the film thickness is not taken into consideration. Also, the experiment results (a) and (b) indicate that the gauge factor increases with grain size reducing at high doping concentration. This conclusion has been explained reasonably by the tunnelling piezoresistive model—because the piezoresistance coefficient π_b is larger than π_g at high doping concentration, the reduction of grain size consequentially results in the increase of grain boundary component, thereby leading the gauge factor to increase.

The experiment results (c) indicated that when the film thickness decreases to 40 nm, the grain size becomes smaller and the gauge factor also decreases. The fact appeared to be opposite to the conclusions from the results (a) and (b); however, it is due to other reasons. In this case, the films are very thin, and the grain growth is not sufficient, causing the increase of trap density at grain boundaries. This increases the weight of equivalent emission resistance so that the piezoresistance coefficient π_b decreases, resulting in the decrease of gauge factor. Additionally, as can be seen from the results (c), when the film thickness is reduced to 30 nm, the grain size becomes much smaller, but the gauge factor increases a little. It should be due

to the change in film nature. On this condition, the apparent grain size is about 15 nm. In view of smaller grains in the deep level of films, it could be considered that the films begin to transfer toward nanocrystalline silicon. The nanocrystalline silicon has a higher gauge factor[26]. However, due to the immature preparation technologies, its piezoresistive properties have not been applied practically for the moment.

6. Conclusions

For polysilicon nanofilms, it was found that the tunnelling piezoresistive effect was quite remarkable. Thus, when the doping concentration exceeds 10^{20} cm^{-3}, the piezoresistance coefficient of composite grain boundaries is larger than that of the grain neutral regions. By comparison between the theory and the experiments, the conclusions were drawn as follows:

At high doping concentrations, polysilicon nanofilms have larger gauge factors than common ones. For the polysilicon nanofilms whose apparent grain size is about 32 nm, when the doping concentration is approximately 4×10^{19} cm^{-3}, the gauge factor has a maximum; after the doping concentration reaches 10^{20} cm^{-3}, the gauge factor increases again with the doping concentration increasing. When the doping concentration reaches 3×10^{20} cm^{-3}, the gauge factor is about 34.

The influence of the film thickness on the gauge factor is quite large, which is only the indirect reason causing the change in gauge factor and it is actually due to the change in grain size and grain boundary state. When the grain boundary states (trap density, grain boundary width, and grain boundary barrier height and so on) are invariable, the gauge factor of polysilicon nanofilms with high doping concentrations increases with the grain size decreasing.

References

[1] Onuma Y, Sekiya K. Piezoresistive properties of polycrystalline thin films. Jpn J Appl Phys, 1974, 11: 420

[2] Mosser V, Suski J, Goss J, et al. Piezoresistive pressure sensors based on polycrystalline silicon. Sensors Actuators A, 1991, 28: 113

[3] Germer W. Microcrystalline silicon thin films for sensor applications. Sensors Actuators, 1985, 7: 135

[4] French P J, Evens A G R. Polycrystalline silicon strain sensors. Sensors Actuators, 1985, 8: 219

[5] French P J, Evens A G R. Piezoresistance in polysilicon and its applications to strain gauges. Solid-State Electron, 1989, 32: 1

[6] Schubert D, Jenschke W, Uhlig T, et al. Piezoresistive properties of polycrystalline and crystalline silicon films. Sensors Actuators, 1987, 11: 145

[7] Kleimann P, Semmache B, Le Berre M, et al. Stress-dependent hole effective masses and piezo- resistive properties of p-type monocrystalline and polycrystalline silicon. Phys Rev B, 1998, 57: 8966

[8] Liu Xiaowei, Wu Yajing, Chuai Rongyan, et al. Temperature characteristics of polysilicon piezoresistive nanofilm depending on film structure. Proceedings of the 2nd IEEE International Nanoelectronics Conference, Shanghai, China, 2008: 1660

[9] Chuai Rongyan, Liu Xiaowei, Huo Mingxue, et al. Influence of doping level on the gauge factor of polysilicon nanofilm. Chinese Journal of Semiconductors, 2006, 27(7): 1230

[10] Mandurah M M, Saraswat K C, Kamins T I. A model for conduction in polycrystalline silicon – Part I: theory. IEEE Trans Electron Devices, 1981, ED-28: 1163

[11] Kamins T I. Hall mobility in chemically deposited polycrystalline silicon. J Appl Phys, 1971, 42: 4357

[12] Taniguchi M, Hirose M, Osaka Y. Substitutional doping of chemically vapor-deposited amorphous silicon. J Cryst Growth, 1978, 45: 126

[13] Liu Xiaowei, Huo Mingxue, Chen Weiping, et al. Theoretical research on piezoresistive coefficients of polysilicon films. Chinese Journal of Semiconductors, 2004, 25: 292

[14] Murphy E L, Good R H. Thermionic emission, field emission and the transition region. Phys Rev, 1956, 102: 1464

[15] Liu Enke, Zhu Bingsheng, Luo Jinsheng. Semiconductor physics. Beijing: Publishing House of Electronics Industry, 2003

[16] Adams E N. Elastoresistance in p-type Ge and Si. Phys Rev, 1954, 96: 803

[17] Pikus G E, Bir G L. Cyclotron and paramagnetic resonance in strained crystals. Phys Rev Lett, 1961, 6: 103

[18] Hensel J C, Feher G. Cyclotron resonance experiments in uniaxially stressed silicon: valence band inverse mass parameters and deformation potentials. Phys Rev, 1963, 129: 1041

[19] Hasegawa H. Theory of cyclotron resonance in strained crystal. Phys Rev, 1963, 129: 1029

[20] Baccarani G, Impronta M, Ricco B, et al. I–V characteristics of polycrystalline silicon resistors. Rev Phys Appl, 1978, 13: 777

[21] Fonash S J. The role of the interfacial layer in metal–semiconductor solar cells. J Appl Phys, 1975, 46: 1286

[22] Lu N C C, Gerzberg L, Lu C Y, et al. Modeling and optimization of monolithic polycrystalline silicon resistors. IEEE Trans Electron Devices, 1981, ED-28: 818

[23] Smith C S. Piezoresistance effect in germanium and silicon. Phys Rev, 1954, 94: 42

[24] Tufte O N, Stelzer E L. Piezoresistive properties of silicon diffused layers. J Appl Phys, 1963, 34: 313

[25] Toriyama T, Sugiyama S. Analysis of piezoresistance in p-type silicon for mechanical sensors. J Microelectromech Syst, 2002, 11: 598

[26] He Yuliang, Liu Hong, Yu Mingbin, et al. The structure characteristics and piezo-resistance effect in hydro-genated nanocrystalline silicon films. Nanostructured Materials, 1996, 7: 769